Available online at www.sciencedirect.com
ScienceDirect
Analytica Chimica Acta 592 (2007) 36–44
ANALYTICA CHIMICA ACTA
www.elsevier.com/locate/aca

Fabrication and characterization of Meldola's blue/zinc oxide hybrid electrodes for efficient detection of the reduced form of nicotinamide adenine dinucleotide at low potential

S. Ashok Kumar, Shen-Ming Chen *

Department of Chemical Engineering and Biotechnology, National Taipei University of Technology, No. 1, Section 3, Chung-Hsiao East Road, Taipei 106, Taiwan, ROC

Received 4 February 2007; received in revised form 3 April 2007; accepted 4 April 2007
Available online 21 April 2007

Abstract

We report the synthesis and the electrochemical properties of hybrid films made of zinc oxide (ZnO) and Meldola's blue dye (MB) using cyclic voltammetry (CV). MB/ZnO hybrid films were electrochemically deposited onto glassy carbon, gold and indium tin oxide-coated glass (ITO) electrodes at room temperature ($25 \pm 2\,^{\circ}C$) from the bath solution containing 0.1 M $Zn(NO_3)_2$, 0.1 M KNO_3 and 1×10^{-4} M MB. The surface morphology and deposition kinetics of MB/ZnO hybrid films were studied by means of scanning electron microscopy (SEM), atomic force microscopy (AFM) and electrochemical quartz crystal microbalance (EQCM) techniques, respectively. SEM and AFM images of MB/ZnO hybrid films have revealed that the surfaces are well crystallized, porous and micro structured. MB molecules were immobilized and strongly fixed in a transparent inorganic matrix. MB/ZnO hybrid films modified glassy carbon electrode (MB/ZnO/GC) showed one reversible redox couple centered at formal potential ($E^{0\prime}$) −0.12 V (pH 6.9). The surface coverage (Γ) of the MB immobilized on ZnO/GC was about 9.86×10^{-12} mol cm^{-2} and the electron transfer rate constant (ks) was determined to be 38.9 s^{-1}. The MB/ZnO/GC electrode acted as a sensor and displayed an excellent specific electrocatalytic response to the oxidation of nicotinamide adenine dinucleotide (NADH). The linear response range between 50 and 300 μM NADH concentration at pH 6.9 was observed with a detection limit of 10 μM (S/N = 3). The electrode was stable during the time it was used for the full study (about 1 month) without a notable decrease in current. Indeed, dopamine (DA), ascorbic acid (AA), acetaminophen (AP) and uric acid (UA) did not show any interference during the detection of NADH at this modified electrode.

Keywords: Meldola's dye; Zinc oxide; Nicotinamide adenine dinucleotide oxidation; Electrocatalysis; Modified electrodes; Sensor

1. Introduction

Nicotinamide adenine dinucleotide (NADH) is one of the most important coenzymes in the human brain and body. This coenzyme is a common cofactor of about 500 dehydrogenases and its reversible regeneration is a key step in the development of amperometric sensors. The electrochemical oxidation of NADH in aqueous solution has attracted considerable interest in order to develop amperometric biosensors for the detection of biomolecules which react under enzymatic conditions with NAD^+ to produce NADH [1,2]. Although the formal potential of the NADH/NAD^+ couple in neutral pH at 25 °C is estimated to be −0.56 V versus SCE, significant overpotential as large as 1.0 V is often required for the direct oxidation of NADH at bare electrodes [3,4]. The electron transfer involves chemical interaction between the electrode surface and the NADH. The oxidative profile and position of the wave point has a critical dependency on pH, buffer system and electrode material [5].

The large overpotential required for the oxidation invites interference from other easily oxidizable species present in the real samples. In addition, the direct oxidation at bare electrodes is often accompanied by the fouling of the electrode surface by the adsorption of reaction intermediates. A way to decrease the high overpotential and avoid the fouling effect is to use a suitable electrocatalyst (mediator) that can facilitate the electron transfer kinetics. In this way, much effort has been made to identify new

* Corresponding author. Tel.: +886 2 27017147; fax: +886 2 27025238.
E-mail addresses: sakumar80@gmail.com (S.A. Kumar), smchen78@ms15.hinet.net (S.-M. Chen).

0003-2670/$ – see front matter © 2007 Elsevier B.V. All rights reserved.
doi:10.1016/j.aca.2007.04.022

materials which can effectively overcome the kinetic barriers for the electrochemical regeneration of NAD^+ [6–13].

Zinc oxide (ZnO) is an important member of the II–VI group of semiconductors. It has applications in optics, optoelectronics, sensors and actuators due to its semiconducting, piezoelectric and pyroelectric properties [14,15]. On the other hand, ZnO is a biocompatible material with a high isoelectric point (IEP) of about 9.5 which make it suitable for absorption of proteins with low IEPs and the protein immobilization is primarily driven by electrostatic interactions [16,17]. Moreover, ZnO nanostructures have unique advantages including the high specific surface area, nontoxicity, chemical stability, electrochemical activity and high electron communication features. Hence, ZnO is promising material for biosensor applications [18]. ZnO films are composed of nanosized metal-oxide particles and have been intensively investigated in recent years for use in self-assembly dye/ZnO thin films [19–22], optoelectronic devices [23–25] and as inorganic acceptor dye-sensitized solar cells [26–28]. ZnO almost exhibits *n*-type conductivity with the electron in its valance band as charge carriers [29]. In ZnO, zinc is acting as deep acceptor and oxygen is acting as deep donor. Recently, we reported the film formation of ZnO with flavin adenine dinucleotide and its interaction with hemoglobin has been studied [30,31].

Among the mediators considered when designing NADH sensors, Meldola's blue dye (MB) is well studied, extensively used compound and being most suitable mediator for facilitating NADH oxidation [32]. This mediator allows to achieve high sensitivity for the amperometric determination of NADH and to detect as low as 2×10^{-6} mol L^{-1} with good selectivity [33]. In recent years the number of reports concerning NADH sensor was continuously increasing and the MB was often a preferred modifier when designing NADH detectors [32,34–36]. Immobilization of MB on SiO_2/Sb_2O_3 binary oxide matrix [34], zirconium phosphate (MB-ZP-CPEs) [35], layered barium and calcium phosphates [36] were reported for fabrication of NADH sensor and their ability to oxidation of NADH have been investigated.

In the present paper, for the first time, we report a new MB/ZnO film modified electrodes preparation and their characterizations by using cyclic voltammetry, electrochemical quartz crystal microbalance (EQCM), scanning electron microscopy (SEM) and atomic force microscopy (AFM), respectively. Electro-deposition of the MB and ZnO onto glassy carbon electrode (GC), indium tin oxide-coated glass (ITO) electrodes and gold-coated quartz crystal were carried out and their ability for electrocatalytic oxidation of NADH was studied. MB/ZnO/GC electrode showed high electrocatalytic activity for NADH oxidation. In addition, chronoamperometric measurement of NADH using the modified electrode has been studied.

2. Experimental

2.1. Reagents and equipment

All chemicals and reagents used in this work were of analytical grade and used as received without further purification. These were: 8-dimethylamino-2, 3-benzophenoxazine (MB, dye content about 90%), reduced form of β-nicotinamide adenine dinucleotide (purity 98%), dopamine hydrochloride (purity 98%) and uric acid (purity 99%) were purchased from Sigma–Aldrich (St. Louis, MO, USA). *p*-acetaminophen (purity 97%), sulfuric acid (H_2SO_4, purity 95%) and sodium hydroxide (NaOH, purity 93%) were purchased from Wako pure chemicals (Osaka, Japan). Ascorbic acid (purity 99%), potassium nitrate, zinc nitrate, sodium acetate (CH_3COONa) and sodium dihydrogen phosphate (NaH_2PO_4) were received from E-Merck (Darmstadt, Germany).

Supporting electrolytes used for electrochemical experiments were 0.1 M H_2SO_4 (pH 1.0), 0.1 M H_2SO_4 + 0.1 M NaOH (for pH 2.0–3.0), 0.2 M CH_3COOH + 0.2 M CH_3COONa (for pH 4.0–5.0) and 0.1 M NaH_2PO_4 + 0.1 M NaOH (for pH 6.0–12.0). The required values of pH solutions were obtained with the described solutions by mixing and the pH of the medium was measured using a Suntex Model SP-701 pH meter (Jiangsu, China).

Before starting electrocatalytic measurements, the stock solution of 10 mM NADH was prepared and then the required quantity of NADH solution was pipette out into the 10 mL of deoxygenated phosphate buffer solution (PBS) (pH 6.9) using micro syringe. The concentrations of added NADH solutions were calculated and the exact concentrations of NADH solutions were also verified by using Hitachi (Hitachi Corporation, Japan) ultra-visible spectrophotometer at 340 nm. The aqueous solutions were prepared using Milli-Q-water and before each experiment the solutions were deoxygenated by purging with pre-purified nitrogen gas.

Electrochemical measurements were performed with CH Instruments (TX, USA) Model-400 potentiostat with conventional three-electrode cell. A BAS glassy carbon and platinum wire are used as the working electrode and counter electrode, respectively. All the cell potentials were measured with respect to an Ag/AgCl [KCl (sat)] reference electrode. Indium tin oxide-coated glass electrodes were purchased from Merck display technologies, ltd (Darmstadt, Germany). ITO thickness and resistance were 30 ± 10 nm and 80 Ω, respectively. Size of the glass: 300 mm × 350 mm × 0.7 mm. Hitachi scientific instruments (London, UK) Model S-3000H Scanning Electron Microscope was used for surface image measurements. The AFM images were recorded with a Multimode Scanning Probe Microscope System operated in tapping mode using model CSPM4000 Instruments, Ben Yuan Ltd. (Beijing, China). All experiments were carried out at room temperature.

2.2. Electro-deposition of MB/ZnO hybrid films

The electro-deposition of MB/ZnO films were carried out from the bath solutions containing 0.1 M $Zn(NO_3)_2$ and 0.1 M KNO_3 with the addition of 1×10^{-4} M MB. The GC electrode or ITO was used as the working electrode with pure platinum wire (99.99%) as the counter electrode and a saturated silver chloride electrode (Ag/AgCl) as the reference electrode. The space width between the working electrode and the counter electrode is less than 1 cm. Prior to the film deposition, the

GC electrode was mechanically polished with alumina powder (Al_2O_3, 0.05 micron) up to a mirror finish and ultrasonicated in distilled water for 2 min. ITO substrates were cleaned by using detergent, diluted hydrochloric acid and then finally rinsed with distilled water. Electro-deposition of MB/ZnO films were deposited onto the above electrodes by sweeping the potential range between 0.3 and −1.3 V (versus Ag/AgCl) at a scan rate of 0.1 V s^{-1} for 10 cycles using consecutive cyclic voltammetry. The as-prepared blue colored films were smooth and strongly adherent to the substrates. Subsequently, they were dried in air for 30 min at room temperature and obtained porous MB/ZnO hybrid films. The thickness of the resulted film could be controlled by increasing or decreasing the number of potential cycles. In the absence of MB in the bath solution, only ZnO films were prepared and investigated for comparison. Effect of dye concentration: The above operating conditions were used for this study with the exception of MB concentration in the bath solution, concentration from 1×10^{-5} to 1×10^{-2} M were used. The results obtained indicate that the change in dye concentration in the specified range has effect on the dye loading with ZnO and it was clear from the surface coverage value was increased with an increase in concentration up to 1×10^{-4} M and thereafter almost no effect on dye loading. For this reason, a concentration of 1×10^{-4} M is used throughout this work.

2.3. Calibration of EQCM

The working electrode for the EQCM measurement was an unpolished AT-cut Au-coated 8 MHz quartz crystals (purchased from CH Instruments). The diameter of the quartz crystal was 13.7 mm and the gold electrode diameter was 5 mm prior to use, the Au-coated quartz crystal surfaces were cleaned by exposure to piranha solution (one part of 30% H_2O_2 in three parts of H_2SO_4) for 2 min, followed by rinsing with pure water and then dried in nitrogen environment. This process was repeated twice. For in situ EQCM experiments one side of the quartz crystal was sealed with a rubber casing, maintaining it in an air environment while the other side was exposed to aqueous solution. The casing is essential for EQCM frequency stability in liquids, the EQCM crystals were used immediately after preparation. Typical EQCM experiments were performed and change in frequency recorded concurrently with the consecutive cyclic voltammograms over scanning cycles between the potentials of 0.3 and −1.3 V at a scan rate of 0.02 V s^{-1}. Sauerbrey's equation (Eq. (1)) is often used to calculate mass loadings in vacuum depositions [37,38].

$$-\Delta f = -\left(\frac{2f_0^2}{A\sqrt{\mu\rho}}\right)\Delta m \quad (1)$$

where A is the piezoelectricity area (0.196 cm^2), ρ the quartz density (2.648 g cm^{-3}), μ the shear modulus (2.947×10^{11} dyne cm^{-2} for AT-cut quartz) and f_0 is the resonance frequency of the quartz crystal can be used to calculate the changes of the mass (Δm) taking place at the electrode surface from the changes of the resonance frequency (Δf) of the quartz crystal. The EQCM was calibrated as described in literature in order to apply Sauerbrey's equation [39]. The mass sensitivity of the crystal is 1.4 ng cm^{-2} Hz^{-1} which was calculated by Sauerbrey's equation.

In order to apply the Sauerbrey's equation for deposition of ZnO, it was verified if the ZnO behaves as a rigid layer. It was done by plotting the mass change upon deposition of the film measured at the cathodic limit versus the charge consumed in the electro-deposition between 0.3 and −1.3 V (versus Ag/AgCl). Assuming that "m" is the mass of deposited ZnO and the charge measured the total amount of deposited film, then this plot should give a straight line with a zero intercept as expected by the Sauerbrey's equation. Linearity was indicated that the mass obtained from the crystal frequency change is only related with the ZnO film growth and does not with the viscoelastic properties of the ZnO film as well as roughness contribution [40,41].

3. Results and discussion

3.1. Fabrication of MB/ZnO/GC hybrid film modified electrodes

Fig. 1 shows the cathodic electro-deposition of MB/ZnO films onto the GC electrode from the bath solutions containing 0.1 M $Zn(NO_3)_2$ and 0.1 M KNO_3 with the addition of 1×10^{-4} M MB by sweeping the potential between 0.3 and −1.3 V for 10 cycles. On the first cathodic scan, a reduction peak of MB was observed at peak potential about −0.10 V, upon scan reversal an oxidation peak was observed at −0.04 V which is the anodic counterpart of the cathodic wave at −0.10 V. The formal potential $E^{0\prime} = (E_{pa} + E_{pc})/2$ of MB reversible redox peak was −0.06 V (pH 5.4). Peak to peak separation (ΔE_p) between cathodic and anodic peak potential was 60 mV. In addition, the cathodic and anodic peak currents at $E^{0\prime}$ −0.06 V increased significantly on the second and subsequent cycles, this behavior was clearly indicated that the deposition of MB dye molecules onto the electrode surface along with ZnO. On the first cycle (see Fig. 1) the peak current of cathodic and anodic waves are not

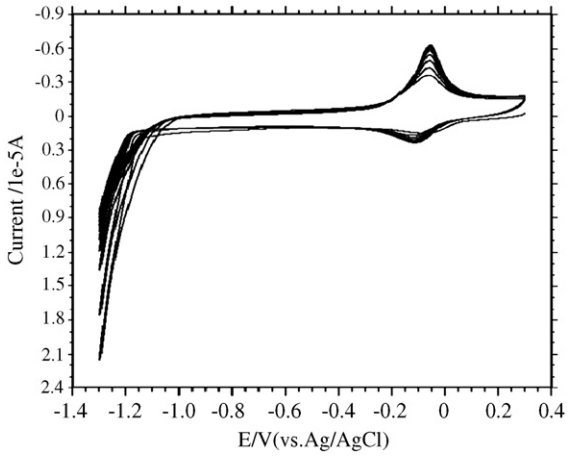

Fig. 1. Cyclic voltammograms of the film growth of MB/ZnO on GC electrode. Electrolyte 0.1 M KNO_3 and 0.1 M $Zn(NO_3)_2$ solution containing 0.1 mM MB. Scan rate = 0.1 V s^{-1}.

equal, the cathodic peak current (I_{pc}) of MB was 1.6 μA and its counterpart anodic peak current (I_{pa}) was 4.3 μA. I_{pc} of MB was 2.7 times lower than the I_{pa}, this difference in peak current indicating that the reduced form of MB strongly adheres to the ZnO surface and it was not released to the solution phase under the operating conditions [22]. In such a way, MB/ZnO/GC hybrid film electrode was prepared and its electrochemical properties were studied.

3.2. Electrochemical behavior of MB/ZnO/GC hybrid film modified electrodes by cyclic voltammetry

The cyclic voltammograms of the MB/ZnO/GC electrode in PBS (pH 6.9) at different scan rates were recorded (Fig. S1A), it showed one reversible redox couple at $E^{0\prime}$ −0.12 V versus Ag/AgCl electrode. The peak currents were proportional to the scan rate up to 200 mV s^{-1} (Fig. S1B) which is an indication of a surface confined redox process. According to the equation, $I_p = n^2F^2\Gamma A\upsilon/4RT$ and $Q_\Gamma = nFA\Gamma$ where n is the number of electrons, A the working electrode area (0.0707 cm^2), υ the scan rate (10 mV s^{-1}) and other parameters have usual meanings [42,43], the electron transfer number and the surface coverage were calculated to be 1.95 and 9.86×10^{-12} mol cm^{-2}, respectively.

The effect of pH on the response of MB/ZnO/GC modified electrode was investigated in the pH range of 1–11 (Fig. S2A). It was found that both the cathodic and anodic peak potentials shifted in a negative direction with increasing pH of the electrolyte solution [44–46]. The $E^{0\prime}$ of the surface redox couple was pH dependent and the $E^{0\prime}$ versus pH plot yields straight line with a slope of 50 mV per unit change in solution pH as shown in the inset of Fig. S2B which was very close to the anticipated Nernstian value (Eq. (2)). It suggests that the overall redox reaction of the film comprises a two-electron and two-proton process. The slope value obtained from $E^{0\prime}$ versus pH plot for surface deposited MB is much closed to the reported values in the literature [34,35,44–46]. pK_a value for MB in the solution phase is not available but it is believed to be similar phenoxazine dyes, (pK_a = 4–5) [47]. These behaviors suggested that the electrochemical process of MB on ZnO proceed with the participation of two hydrogen ions. Collectively the electrode reaction of the MB/ZnO/GC can be presented as follows [34,35]

$$MB + 2H^+ + 2e^- \leftrightarrow MBH_2 \quad (2)$$

Since, the electroactive species is found entrapped in the ZnO matrix pores, the kinetic evaluation of the redox process at the electrode-solution interface is very important. At higher sweep rates ($\upsilon > 200$ mV s^{-1}) peak separations begin to increase indicating the limitation due to charge transfer kinetics. Based on Laviron theory [48] the ks value can be determined by measuring the variation of peak potential with scan rate. The values of peak potentials were proportional to the logarithm of the scan rate higher than 1.0 V s^{-1} (Fig. 2). The slope value of the ΔE_{pc} versus log(υ) was about 170 mV for MB and the charge transfer coefficient (α) value was 0.5, introducing these values

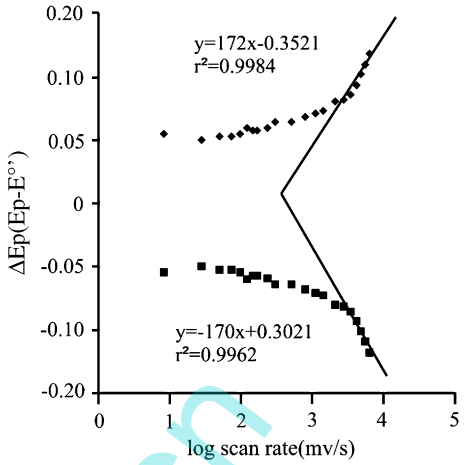

Fig. 2. Plot of peak potential separation vs. log υ for MB/ZnO/GC hybrid films.

in Eq. (3) [49]

$$\log ks = \alpha \log(1-\alpha) + (1-\alpha)\log \alpha - \log\left(\frac{RT}{nF\upsilon}\right) - \frac{\alpha(1-\alpha)nFE}{2.3RT} \quad (3)$$

An apparent surface ks value 38.9 s^{-1} was estimated for reversible redox peak of MB on ZnO/GC modified electrode. This ks value is one order of magnitude higher than literature reported value for MB in SiO_2/TiO_2/phosphate modified carbon paste electrode [44] which is indicating high ability of ZnO for promote electron between MB and electrode surface.

3.3. EQCM study for MB/ZnO hybrid film deposition and in situ mass measurements

The EQCM is a powerful instrument that is capable of detecting very small mass changes on the gold electrode's surface that accompanies the electrochemical process occurring on the electrode surface. The EQCM combined with cyclic voltammetry was used to study the "in situ growth" of the MB/ZnO films formation onto gold-coated quartz crystal from the bath solutions containing 0.1 M $Zn(NO_3)_2$, 0.1 M KNO_3 and 1×10^{-4} M MB by sweeping the potential range between 0.3 and −1.3 V (pH 5.4). Fig. 3a demonstrates that the corresponding mass changes in the EQCM recorded during the first five cycles of the consecutive cyclic voltammetry. The increases in the mass noticed in Fig. 3a are found consistent with the growth of ZnO/MB film onto the gold electrode. These results confirmed that the deposition potential for ZnO/MB film formation mainly occurred between −0.6 and −1.3 V (versus Ag/AgCl).

As can be seen in Fig. 3, the mass begin to increase at (above −0.6 V) the same region of the large cathodic currents was seen in cyclic voltammogram at the end of the negative scan due to the reduction of nitrate ions (see Fig. 1). Nitrate ions are reduced to nitrite ions liberating OH^- ions. As a result deposition of ZnO occurs on electrode surface [50] and the simultaneous co-deposition of MB molecules were also occurred. In order to

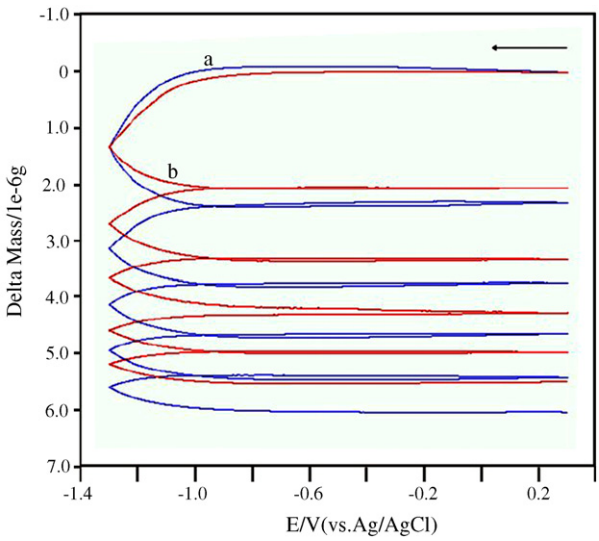

Fig. 3. (a) Changes in mass with respect to MB/ZnO film formation (blue line) during five consecutive cycles in 0.1 M KNO_3, 0.1 M $Zn(NO_3)_2$ and 0.1 mM MB solution and (b) changes in mass with respect to ZnO film formation (red line) during five consecutive cycles in 0.1 M KNO_3 and 0.1 M $Zn(NO_3)_2$ solution on gold-coated quartz crystal electrode. Scan rate = 20 mV s^{-1}.

understand the adsorption mechanism of MB on ZnO surface, in the absences of MB in the bath solution only ZnO film deposition was carried out onto gold crystal [19–22,50] and the corresponding mass change was measured by EQCM technique, results are presented in Fig. 3b (red line).

In order to compare MB/ZnO and only ZnO film growth mechanism, the EQCM experimental results were compared for first five cycles (Fig. 3). For the first cathodic scan during MB/ZnO film deposition, the mass was increased about 2.323 μg and the total mass change for five cycles was 6.028 μg (Fig. 3a). On other hand, only ZnO film formation also occurred mainly between the potential ranges of −0.6 and −1.3 V, but the mass change due to the ZnO film deposition in the absences of MB for first cathodic scan was 2.054 μg and the total mass change after five cycles was about 5.501 μg. The total difference in mass between MB/ZnO and only ZnO film deposition was 0.527 μg for five cycles; this difference in mass may arose due to the co-deposition of dye molecules with ZnO onto gold crystal surface. These results clearly suggested that the deposition of ZnO/MB was occurred mainly in the potential range between −0.6 and −1.3 V.

Film thickness of MB/ZnO was controlled by the number of CV cycles during the cathodic deposition and the corresponding surface coverage's were calculated by using the equation $\Gamma = Q/nFA$, it was interesting to observe that there was a rapid increase in surface coverage of MB for up to ten cycles. After the tenth cycles, the surface coverage slowly tended to reach the limiting value. Hence, in the present investigation the MB/ZnO film thickness was controlled by the number of cycles using CV. However, the thickness of the MB/ZnO and only ZnO films were measured using AFM technique (Fig. 4) and the film thicknesses were found to be 1.1 ± 1 and 0.4 ± 0.1 μm for MB/ZnO and only ZnO films after ten cycles, respectively.

3.4. AFM and SEM analysis of MB/ZnO and ZnO films

Fig. 4 shows the surface topography of the (A) ZnO and (B) MB/ZnO hybrid films. As we seen in Fig. 4A, the brighter particles were thought to be ZnO with an average particle size between 200 and 400 nm and the film thickness was about 0.4 ± 0.1 μm. The surface image of only ZnO film shows the small gabs between ZnO particles. Furthermore, Fig. 4B shows the surface topography of the MB/ZnO hybrid films and the particles size of the MB/ZnO hybrid films were between 600 and 957 nm with an average film thickness of 1.1 ± 1 μm. When compare Fig. 4A and B, it was understood in the presence of dye molecules in the bath solution, the particles size and the film growth of ZnO highly affected and the MB molecules were strongly adsorbed with ZnO film. In addition, the thickness of the MB/ZnO hybrid film is significantly larger than that of the ZnO films alone. This is an indication of good interaction between the MB and ZnO. The randomly oriented ZnO particles were consistently covered with MB molecules and this porous morphology allows for excellent electrolyte access with less resistance. The high conductivity of ZnO film increases the electrical properties of the redox processes and also provides a large surface area available for MB intercalation.

SEM images of ZnO shows the plate-like structures (Fig. 5A). Yoshida et al. reported that the dye stuffs, such as eosin Y and tetrabromophenol significantly altered the surface morphology of ZnO when they were present in the bath solution at even low concentration results colored ZnO thin films with totally different surface morphologies and crystallographic structures

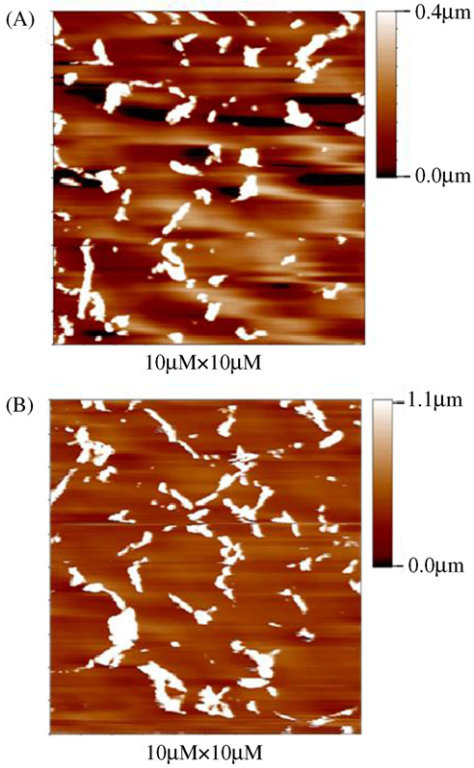

Fig. 4. AFM image of (A) ZnO film and (B) MB/ZnO hybrid film.

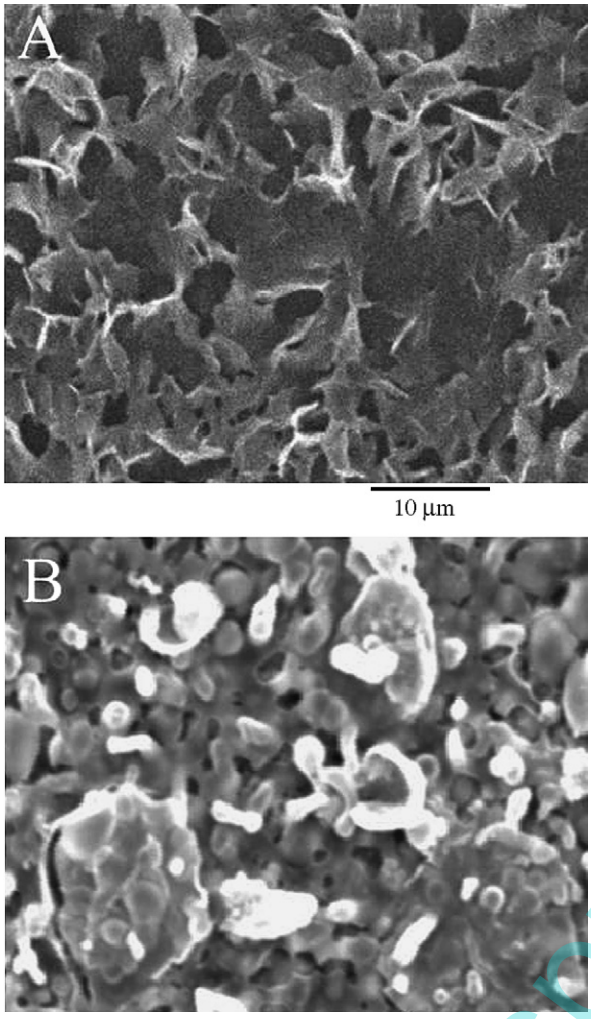

Fig. 5. SEM image of (A) ZnO film and (B) MB/ZnO hybrid film.

from the pure ZnO film. In many cases surface adsorption of dye molecules hinders crystal growth leading to automatic formation of porous thin films composed of nanosized crystallites of ZnO suitable for the dye-sensitized solar cells [21,22]. MB molecules also highly altered the surface morphology of ZnO (Fig. 5B) and highly porous surfaces were obtained. Evidently ZnO particles are covered by a layer of organic dye film suggesting that MB has been adsorbed on the surface of ZnO particles.

In the control experiment, GC electrode was cycled between 0.3 and −1.3 V for 10 cycles in the solutions containing 0.1 M KNO_3 and 1×10^{-4} M MB, it was noted that the redox peak current of MB was decreased, however some of the dye molecules physically adsorbed onto GC electrode surface [51,52]. Thereafter, GC electrode was transferred into PBS, physically adsorbed dye molecules were shown a reversible redox wave but the peak current was diminished after few cycles, it was indicating that leaching of dye molecules from the electrode surface. However, in the case of hybrid film, the stability of MB/ZnO/GC hybrid film modified electrode was tested by continuous potential sweeping at 50 mV s^{-1} between −0.5 and 0.2 V in 0.1 M PBS (pH 6.9). An insignificant decay in the peak currents was observed during the initial cycles (2% for first 25

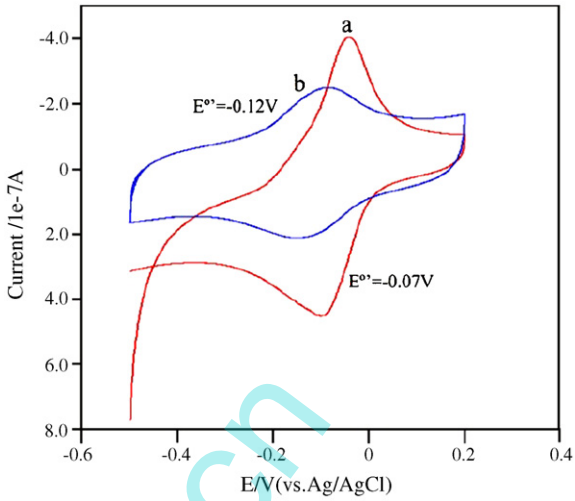

Fig. 6. Cyclic voltammograms of (a) 0.1 mM MB in pH 6.9 PBS at bare GC electrode and (b) MB/ZnO/GC modified electrodes in pH 6.9 PBS. Scan rate = 10 mV s^{-1}.

cycles) and the rate of current decrease then decreased (only 4% after 200 cycles). This test clearly showed that the MB/ZnO/GC hybrid film electrode has good stability.

Fig. 6a shows the cyclic voltammogram of MB/ZnO/GC electrode in PBS, the $E^{0\prime}$ value for redox MB peak on ZnO/GC electrode was −0.12 V. This value is shifted towards more negative potentials when compared to those observed for soluble MB species in solution (−0.07 V) (Fig. 6b). This shift in $E^{0\prime}$ value between MB/ZnO/GC and MB in solutions indicates that the reduced form of dye much more strongly interacts with the ZnO matrix like eosin Y [22].

3.5. Electrocatalytic oxidation of NADH

The cyclic voltammograms were recorded at 10 mV s^{-1} by using MB/ZnO/GC modified electrode in the absence and presence of 15, 30 and 45 μM NADH as shown in Fig. 7. All these experiments were performed in the absence of light. The greatly enhanced oxidation current at 0.0 V shows that the modified electrode could catalyze the oxidation of NADH effectively. It was obvious that NADH diffuses to the electrode surface and reacts with the oxidized forms of MB. Thus, a large increase of current resulting from the re-oxidation of MB can be obtained. In comparison with the results obtained at a bare GC electrode, in which the potential for the oxidation of NADH is about 0.6 V, hence, this modified electrode lowered the anodic overpotential of NADH by about 600 mV. The reaction process can be expressed as [44–46]

$$\text{NADH} + \text{MB(oxidizedform)} \rightarrow \text{NAD}^{+} + \text{MB(reducedform)} \quad (4)$$

In addition when MB/ZnO/GC modified electrode was immersed in PBS containing 50 μM NADH for an hour and then the electrode was thoroughly washed by using doubly distilled water. Thereafter, cyclic voltammogram was recorded using the above immersed electrode in PBS, no obvious change in the

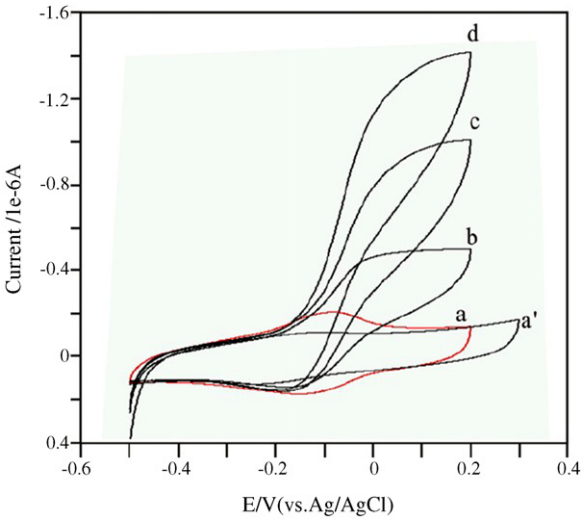

Fig. 7. Cyclic voltammograms of MB/ZnO/GC modified electrodes in pH 6.9 PBS: NADH = (a) 0.0 μM, (b) 15 μM, (c) 30 μM, (d) 45 μM and (a′) bare GC electrode with 45 μM NADH. Scan rate = 10 mV s^{-1}.

voltammogram was observed before and after immersion. All these results suggested that MB/ZnO/GC modified electrode does not suffer from the problem of electrode poisoning. The oxidation of NADH is a two-electron process at MB/ZnO/GC modified electrodes [44–46].

The amperometric response of the MB/ZnO/GC modified electrode for the measurements of NADH has been examined. The chronoamperogram was obtained in a series of concentrations of NADH at 0.0 V and the results are shown in Fig. 8. Upon the addition of 50 μM NADH, the MB/ZnO/GC electrode responds favorably to each of the addition, yielding steady state signals within 2 s. These data indicates that the MB/ZnO/GC sensor has a higher electrocatalytic activity for NADH oxidation.

A calibration curve of current (*I*) versus concentrations (*c*) for NADH was obtained at this modified electrode. The dependence of current response on the concentration of NADH was

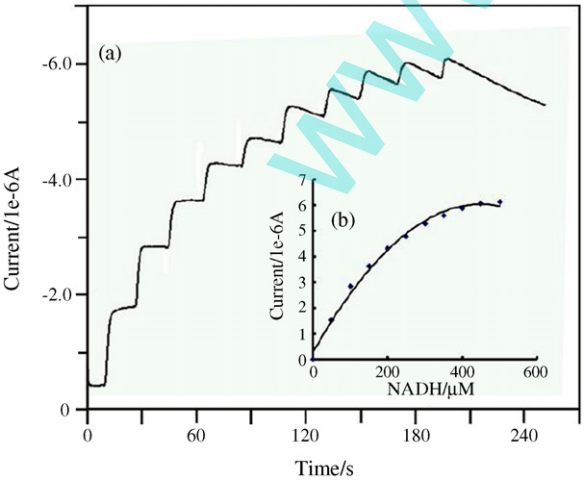

Fig. 8. Typical amperometric curve obtained with a MB/ZnO/GC electrode in 0.1 M phosphate buffer solution (pH 6.9) at an applied potential of 0.0 mV s^{-1} vs. Ag/AgCl, stirring rate ~300 rpm. (a) Successive additions of 50 μM NADH solution and (b) the corresponding standard addition plots.

linear in the range from 50 to 300 μM, after this linear range the current attained steady state. In order to further investigate reproducibility and to estimate the limit of detection (LOD) of the proposed method, various concentrations of aqueous NADH solutions were prepared, analyzed through the MBO/ZnO sensor by amperometric technique, and also spectroscopically analyzed after a measurement time of 1 min at 340 nm. Spectroscopic studies of NADH solutions were carried out in dark condition. The mean and standard deviation of repeated measurements in a concentration range of 50–300 μM were determined and plotted versus input concentrations (inset Fig. 8). All peak height values fit a linear regression function with a correlation coefficient of 0.9951 and standard deviation of 0.1157. The standard addition data showed that the LOD was 10 μM at a signal-to-noise ratio (S/N) of 3.

The MB/ZnO/GC modified electrode not only showed significant catalytic activity towards NADH oxidation but also exhibited good antifouling properties for NADH and its oxidation byproducts. Also, to study the repeatability of the modified electrode response for the electrocatalytic oxidation of NADH, nine times 50 μM NADH solutions were injected into the buffer solution and their catalytic current were measured at 0.0 V. It was found that the relative standard deviation (R.S.D.) was 3.92% (Table S1). Herein, the reported experiments prove that no accumulation of analyte molecules takes places within the ZnO matrix even after several measurement cycles.

Cyclic voltammograms of MB/ZnO/GC modified electrode was recorded before and after the immersion of the electrode in PBS for a month, the shape and peak current of the both voltammograms were almost the same. This test clearly indicated that this modified electrode has good stability and MB molecules were not easily leached out from the ZnO surface, hence this modified electrode may be very useful for detection of NADH.

In addition, catalytic current response for NADH oxidation at MB/ZnO/GC electrode was tested in the solution containing 50 μM NADH before and after continuous stirring the buffer solution for 30 min. The response of the electrode signal had no change for both case, this test indicated that reproducible results can be obtained at MB/ZnO/GC modified electrode. Moreover, this method compares reasonably well with other techniques utilizing MB as an electron transfer mediator [34–36,45,46] and it can be envisaged that this maybe improved by increasing the loading of the ZnO upon the electrode surface. The linear range of NADH detection at ZnO/MB/GC electrode is compared with the earlier literature report in Table 1.

3.6. Effect of interference study on electrode response

The effect of interferences on the analytical response of MB/ZnO/GC hybrid electrode has been studied. This was initiated by studying the hydrodynamic voltammetric response as a means of determining the effect of interference for the amperometric detection of NADH. DA, AA, AP and UA are the most important interferences in biological samples. Moreover, at bare electrodes, the oxidation of DA, AA, AP and UA occurred at a potential close to that of NADH [2,53,54]. Therefore, it is very important to separate the oxidation potentials of NADH

Table 1
Comparison of MB/ZnO/GC electrode system with other reported methods for NADH oxidation

Modified electrodes	Linear range (mol L^{-1})	Oxidation potential (V)	Reference
SNMB	1×10^{-5} to 7.5×10^{-4}	0.0	[45]
SiSb/MB	1×10^{-4} to 6.0×10^{-4}	0.0	[34]
STPM-MB	1×10^{-5} to 5×10^{-5}	0.0	[46]
MB/ZnO	5×10^{-5} to 3.0×10^{-4}	0.0	tw

SNMB: Meldola's blue dye adsorbed on silica gel coated with niobium oxide; SiSb/MB: MB adsorbed on SiO_2/Sb_2O_3 oxide matrix; STPM-MB: MB adsorbed on titanium phosphate coated on a silica gel surface; tw: this work.

from the above interferences. In order to overcome the above-mentioned problems, bioelectrochemists and electroanalytical chemists have shown great interest in this area and various modified electrodes have been constructed for this purpose [2,54].

In this experiment the potential was kept at 0.0 V, the voltammetric response for the successive additions of 0.5 mM DA, 0.5 mM AP, 0.5 mM AA at MB/ZnO/GC modified electrode were recorded, it was observed that these interferences not shown any response at this modified electrode. Indeed, 50 μM NADH was added into the same buffer solution, MB/ZnO/GC modified electrode reveals an oxidative current which rises sharply and then 0.5 mM UA solution was added into the electrolyte there is no any response at MB/ZnO/GC hybrid electrode for UA also and then further addition of 50 μM NADH shown a stable same response again (Fig. 9). These results clearly indicated that DA, AP, AA and UA did not interfere in the steady state current of NADH at 0.0 V. This result is qualitatively consistent with the cyclic voltammetric data presented in Fig. 7, in which the NADH oxidation wave emerges at 0.0 V. The lowering in the detection potential for the hydrodynamic voltammetry can be tentatively attributed to the NADH catalytically reducing the monomer of MB, thereby producing a catalytic enhancement in the monomer oxidation wave. As expected from the voltammetric profiles, the unmodified GC electrode did not display any signals over the range of 50–300 μM NADH.

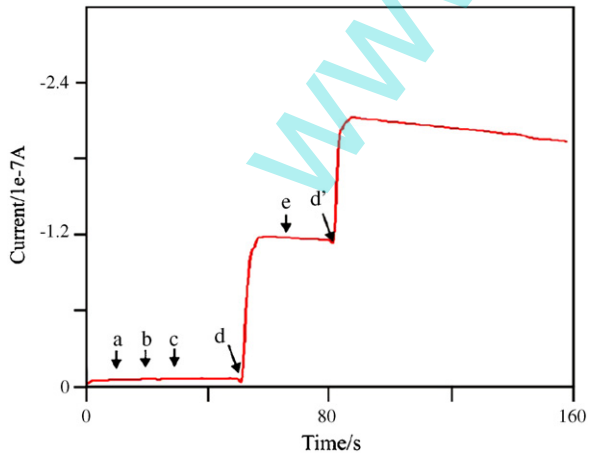

Fig. 9. Typical amperometric curve obtained with a MB/ZnO/GC electrode in 0.1 M phosphate buffer solution (pH 6.9) at an applied potential of 0.0 mV s^{-1} vs. Ag/AgCl, stirring rate ~300 rpm. Successive additions of (a) 0.5 mM dopamine, (b) 0.5 mM acetaminophen, (c) 0.5 mM ascorbic acid, (d, d′) 17 μM NADH and (e) 0.5 mM uric acid solutions.

The zero-point charge (zpc) for ZnO is 9.0. Based on the pHzpc value, ZnO surface is positively charged at below pH 9 [18,55]. At low pH value electrostatic interactions between the positive ZnO surface and dye anions [MB^-] in aqueous solutions may be lead to strong adsorption of the dye on the ZnO surface. Fouad et al. reported that the same observation for C.I. Reactive Black 5 dye on ZnO [55]. Presumably the reduced form of the adsorbed dye is more stabilized inside the matrix pores. Since MB molecules are also strongly entrapped inside the matrix pores. They are not leached from the surface easily in the pH 6.9 PBS and also they are not affected by the external solution pH change. These reasons contribute to the high stability and high affinity of the sensor constructed by ZnO as a matrix and it was successfully used for the measurement of NADH at low potential.

4. Conclusions

In summary, we reported a new sensor by immobilized MB on the crystalline ZnO for NADH detection at 0.0 V. SEM and AFM images of MB/ZnO hybrid films have revealed that the surfaces are well crystallized, porous and micro structured. MB molecules were immobilized and strongly fixed in a transparent inorganic matrix. The MB/ZnO/GC electrode acted as a sensor and displayed an excellent specific electrocatalytic response for the measurement of NADH and a good linear response observed in the range from 50 to 300 μM with a detection limit of 10 μM (S/N = 3). Moreover, the electrode found to be very stable for more than 1 month. DA, AP, AA and UA did not show any interference during the measurement of NADH.

The above results showed that the ZnO formed an attractive matrix for MB immobilization. This is the very simple method for electrode fabrication and it can be very useful for detection of NADH in real samples also.

Acknowledgements

This project work was financially supported by the Ministry of Education and the National Science Council of Taiwan, ROC.

Appendix A. Supplementary data

Supplementary data associated with this article can be found, in the online version, at doi:10.1016/j.aca.2007.04.022.

References

[1] A.P.F. Turner, I. Karube, G.S. Wilson (Eds.), Biosensors—Fundamentals and Applications, Oxford University Press, New York, 1987.
[2] L. Gorton, E. Dominguez, Electrochemistry of NAD(P)$^+$/NAD(P)H, encyclopedia of electrochemistry, in: G.S. Wilson (Ed.), Bioelectrochemistry, vol. 9, Wiley-VCH, Weinheim, 2002.
[3] J. Moiroux, P.J. Elving, Anal. Chem. 50 (1978) 1056.
[4] L. Gorton, G. Johansson, A. Torstensson, J. Electroanal. Chem. 196 (1985) 81.
[5] W. Blaedel, R. Jenkins, Anal. Chem. 47 (1975) 1337.
[6] F.D. Munteanu, N. Mano, A. Kuhn, L. Gorton, Bioelectrochemistry 56 (2002) 67.
[7] N. Mano, A. Kuhn, Electrochem. Commun. 1 (1999) 497.
[8] P.N. Bartlett, E. Simon, C.S. Toh, Bioelectrochemistry 56 (2002) 117.
[9] P.N. Bartlett, E.N.K. Wallace, J. Electroanal. Chem. 486 (2000) 23.
[10] P.N. Bartlett, E. Simon, J. Am. Chem. Soc. 125 (2003) 4014.
[11] A.A. Karyakin, Y.N. Ivanova, K.V. Revunova, E.E. Karyakina, Anal. Chem. 76 (2004) 2004.
[12] J. Wang, L. Anges, T. Martinez, Bioelectrochem. Bioenerg. 29 (1992) 215.
[13] N.S. Lawrence, J. Wang, Electrochem. Commun. 8 (2006) 71.
[14] D.P. Norton, Y.W. Heo, M.P. Ivill, S.J. Pearton, M.F. Chisholm, T. Steiner, Mater. Today 7 (2004) 34.
[15] X.W. Sun, H.S. Kwok, J. Appl. Phys. 86 (1999) 408.
[16] F.F. Zhang, X.L. Wang, S.Y. Ai, Z.D. Sun, Q. Wan, Z.Q. Zhu, Y.Z. Xian, L.T. Jin, K. Yamamoto, Anal. Chim. Acta 519 (2004) 155.
[17] Z.M. Liu, Y.L. Liu, H.F. Yang, Y. Yang, G.L. Shen, R.Q. Yu, Electroanalysis 17 (2005) 1065.
[18] J.X. Wang, X.W. Sun, A. Wei, Y. Lei, X.P. Cai, C.M. Li, Z.L. Dong, Appl. Phys. Lett. 88 (2006) 233106.
[19] T. Yoshida, D. Komatsu, N. Shimokawa, H. Minoura, Thin Solid Films 66 (2004) 451.
[20] M. Izaki, T. Omi, Appl. Phys. Lett. 68 (1996) 2439.
[21] S. Karuppuchamy, T. Yoshida, T. Sugiura, H. Minoura, Thin Solid Films 397 (2001) 63.
[22] T. Yoshida, H. Minoura, Adv. Mater. 12 (2000) 1219.
[23] A. Petrella, P.D. Cozzoli, M.L. Curri, M. Striccoli, P. Cosma, A. Agostiano, Bioelectrochemistry 63 (2004) 99.
[24] A.D. Schlettwein, T. Oekermann, T. Yoshida, M. Tochimoto, H. Minoura, J. Electroanal. Chem. 481 (2000) 42.
[25] A.K. Keis, E. Magnusson, H. Lindstrom, S.-E. Lindquist, A. Hagfeldt, Sol. Energy Mater. Sol. Cells 73 (2002) 51.
[26] L. Bahadur, P. Srivastava, Sol. Energy Mater. Sol. Cells 79 (2003) 235.
[27] H. Rensmo, K. Keis, H. Lindstrom, S. Sodergren, A. Solbrand, A. Hagfeldt, S.-E. Lindquist, J. Phys. Chem. B 101 (1997) 2598.
[28] G.C. Van de Walle, Phys. Rev. Lett. 85 (2000) 1012.
[29] C.H. Farr, J. ACAM 1 (1998) 113.
[30] K.C. Lin, S.M. Chen, J. Electroanal. Chem. 578 (2005) 213.
[31] K.C. Lin, S.M. Chen, Biosens. Bioelectron. 21 (2006) 1737.
[32] A. Vasilescu, S. Andreescu, C. Bala, S.C. Litescu, T. Noguer, J.-L. Marty, Biosens. Bioelectron. 18 (2003) 781.
[33] J. Wang, P.V.A. Pamidi, M. Jiang, Anal. Chim. Acta 360 (1998) 171.
[34] E.S. Ribeiro, A.S.S. Rosatto, Y. Gushikem, A.L.T. Kubota, J. Solid State Electrochem. 7 (2003) 665.
[35] C.I. Ladiu, I.C. Popescu, L. Gorton, J. Solid State Electrochem. 9 (2005) 296.
[36] A.M. Lazarin, C. Airoldi, Sens. Actuator B 107 (2005) 446.
[37] G. Sauerbrey, Z. Phys. 155 (1959) 206.
[38] V. Tsionsky, L. Daikhin, M. Urbakh, E. Gileadi, in: A.J. Bard, I. Rubinstein (Eds.), Electroanalytical Chemistry, vol. 22, Marcel Dekker, New York, 2004, pp. 1–99.
[39] L.M. Abrantes, C.M. Cordas, E. Vieil, Electrochim. Acta 47 (2002) 1481.
[40] H. Varela, R.M. Torresi, D.A. Buttry, J. Electrochem. Soc. 147 (2000) 4217.
[41] A. Bund, M. Schneider, J. Electrochem. Soc. 149 (2002) E331.
[42] A.J. Bard, L.R. Faulkner, Electrochemical Methods Fundamentals and Applications, Wiley, New York, 1980, pp. 521–525.
[43] A.P. Brown, F.C. Anson, Anal. Chem. 49 (1977) 1589.
[44] C.U. Ferreira, Y. Gushikem, L.T. Kubota, J. Solid State Electrochem. 4 (2000) 298.
[45] A.S. Santos, L. Gorton, L.T. Kubota, Electroanalysis 14 (2002) 805.
[46] L.T. Kubota, F. Gouvea, A.N. Andrade, B.G. Milagres, G.D.O. Neto, Electrochim. Acta 41 (1996) 1465.
[47] E. Bishop, Indicators, in: R. Belcher, H. Frieser (Eds.), International Series of Monographs in Analytical Chemistry, vol. 51, Pergamon Press, Oxford, 1972.
[48] E. Lavion, J. Electroanal. Chem. 101 (1979) 19.
[49] E. Laviron, J. Electroanal. Chem. 52 (1974) 355.
[50] S. Otani, J. Katayama, H. Umemoto, M. Matsuoka, J. Electrochem. Soc. 153 (2006) C551.
[51] Y. Zhu, S. Dong, Electrochim. Acta 35 (1990) 1139.
[52] L. Mao, J. Jin, L. Song, K. Yamamoto, L. Jin, Electroanalysis 11 (1999) 499.
[53] H.R. Zare, N. Nasirizadeh, M.M. Ardakani, J. Electroanal. Chem. 577 (2005) 25.
[54] P.N. Bartlett, E.N.K. Wallace, Phys. Chem. Chem. Phys. 3 (2001) 1491.
[55] O.A. Fouad, A.A. Ismail, Z.I. Zaki, R.M. Mohamed, Appl. Catal. B-Environ. 62 (2006) 144.